Active MHD Instability Control and Confinement in the TPE-RX RFP

H. Sakakita 1), A. M. Canton 2), B. E. Chapman 3), K. Hayase 1), Y. Hirano 1),
P. Innocente 2), S. Kiyama 1), H. Koguchi 1), J. S. Sarff 3), Y. Sato 1), S. Sekine 1),
T. Shimada 1), Y. Yagi 1)

1) National Institute of Advanced Industrial Science and Technology (AIST), Tsukuba, Japan
2) Consorzio RFX, Padua, Italy
3) University of Wisconsin - Madison, Wisconsin, USA

e-mail contact of main author: h.sakakita@aist.go.jp

Abstract. Experimental results obtained by using active methods to control the locked mode and to improve the confinement in the TPE-RX (R/a = 1.72/0.45) reversed field pinch (RFP), are presented. A phase- and wall-locked mode (LM) was found in the case of high plasma current (> 300 kA) and/or high filling pressure. The rotation of the LM has been attempted by using an auxiliary rotating toroidal magnetic field. By applying the auxiliary field, the LM can be successfully delayed or even eliminated in the case of plasma current less than 250 kA. Double-pulse pulsed poloidal current drive (PPCD) has been conducted by using the auxiliary and main reversal toroidal field systems. The electron temperature, density and ion temperature increase during the PPCD. The result of the double-pulse PPCD is a fivefold increase in energy confinement time (τ_E) compared to that of the standard case. Moreover, the five-pulse PPCD result indicates the further improvement of poloidal beta (β_P) and τ_E compared to the double-pulse PPCD. The high electron density discharges are obtained by using fast gas puffing. The higher values of β_P and τ_E are realized in the highest electron density case. A neutral beam injection has been tested for another active control of the RFP plasma.

1. Introduction

Current main issues associated with the reversed field pinch (RFP) experiments are the improvement of the confinement characteristics by the control of magnetohydrodynamic (MHD) instabilities such as dynamo activities, and the establishment of those control methods. TPE-RX is a large RFP (R/a = 1.72/0.45 m, R and a are major and minor radii) with a multilayered shell system which has the capability of equilibrium control up to the designed maximum plasma current, I_P of 1MA, and a shell proximity of b/a = 1.08 (b is the minor radius of the innermost shell) [1]. The vacuum vessel is made of 316L stainless steel with fixed molybdenum limiters. The maximum I_P and pulse duration time, τ_d, of 0.48 MA and 0.1 s, respectively, have been separately attained. Global confinement properties of TPE-RX for discharges without active controls were reported at the last IAEA conference [2]. In this report, experimental results using active methods, such as the control of the toroidal magnetic field and gas puffing to control the locked mode and to improve the confinement, are described.

2. Experimental Results

2.1. TPE-RX RFP

One of the most unique features in the TPE-RX is its equilibrium system for canceling the poloidal shell gap error and for controlling the plasma horizontal displacement. The equilibrium system consists of double layered thin copper shells, a thick aluminum single shell, primary vertical field, control vertical field, saddle coil field, quasi-DC vertical field and pulsed vertical field [3]. Experiments have usually been conducted without the quasi-DC vertical field. To reduce the necessary strength of the DC vertical field for centering the plasma in the vacuum vessel, the center of the vacuum vessel is shifted by 17.5 mm in the outer direction of the torus with respect to the center of the thick shell. The basic performance of the TPE-RX was first reported in Ref. [4]. Global confinement properties under the standard operating conditions, at I_P < 0.5 MA, give the range of poloidal beta, β_P = 5-10 %, and the energy confinement time, τ_E = 0.5-1 ms with the relatively high I_P/N value (N =

$\pi a^2 \langle n_e \rangle$, $\langle n_e \rangle$ is the volume averaged electron density) of 12 x 10^{-14} Am [2]. The standard operating conditions are characterized by a pinch parameter (Θ) ~1.4-1.5, feedback-controlled gap-error field compensation, equilibrium maintained by the thick conductive shell and fueling with a semi-steady flow of deuterium. In the following section, experimental results obtained by using several active control methods are presented.

2.2. Control of the Locked Mode

It is found in the TPE-RX, that the phases of several toroidal Fourier modes mutually align and form toroidally localized magnetic fluctuations (phase locking), which sometimes remain in a certain location of the torus (wall locking) [5]. Hereafter, we call this the locked mode (the LM) that locks in both phase and wall. The LM is always observed in the case of high I_P (> 300 kA) and/or a high filling pressure for the deuterium gas (P_{D2}). Since a strong plasma-wall interaction is caused, the LM contaminates the plasma through spattered impurities and limits the high I_P operation [5]. To control the LM, a similar method as was used in RFX RFP [6] has been attempted. A rotating toroidal magnetic field (B_{Trot}) is produced by an auxiliary toroidal field system, which consists of 16 additional auxiliary toroidal field coils and 16 independent power supplies. In a typical condition with 5 ms pulse width and 9.6 ms rotation period, the main rotating component of the applied field without the plasma is $m = 0 / n = 1$ with a maximum amplitude of ~2.5 mT. Here, m and n represent the poloidal and toroidal mode numbers, respectively. In an example of low I_P (200 kA) with high P_{D2} (0.8 mTorr) as shown in FIG. 1(a), the LM is observed from t ~20 ms and at the toroidal angle of 280 degrees without B_{Trot}. By applying B_{Trot}, the LM can be successfully delayed or even eliminated in some cases as shown in FIG. 1(b). To obtain this result, both an early start (t < ~12.5 ms, before the LM occurs) and a fast rotation speed (< ~20 ms/rotation) of B_{Trot} are required. However, once the LM appears, it is difficult to unlock it by B_{Trot} in TPE-RX. On the other hand, in RFX, the LM can be driven to rotate by B_{Trot}, but cannot be eliminated.

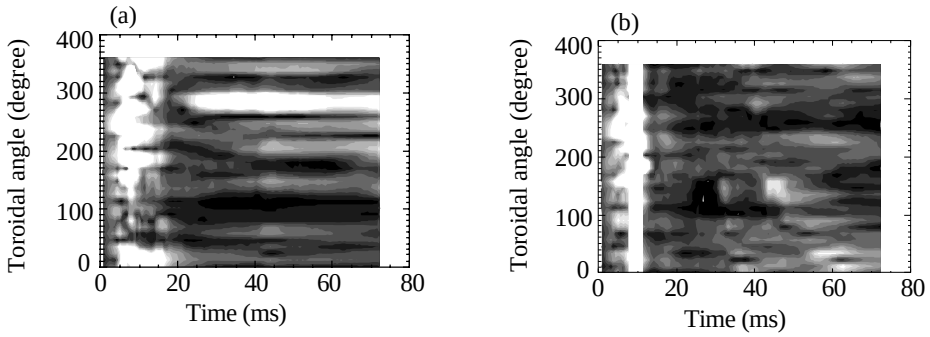

FIG. 1. Shift of last closed flux surface as a function of time and toroidal angle. (a) Locked mode case, (b) controlled unlocking case.

B_{Trot} is applied from t ~30 ms to the discharges of I_P = 250 kA, in which the LM takes place at t ~35 ms. Figure 2 shows phase dispersions (ψ) at several time points with and without B_{Trot}. The phase dispersions are defined by an equation, $\psi = (1/N_{j\,k}) \Sigma_j \Sigma_k \left| \sin\{(j\,\phi + \alpha_j - k\,\phi - \alpha_k)/2\} \right|$. Here, ϕ denotes the toroidal angle and α_j denotes the phase of $m = 0$ or $1 / n = j$ modes. Here, we take j, k = 1-15. The phase dispersion becomes zero, when the phases of all modes are completely locked [7]. The unlocking of the phase in both $m = 0$ and $m = 1$ modes is observed with the B_{Trot} case. Figure 3 shows phase variations with and without B_{Trot}. The $m = 0 / n = 1$ mode, and possibly the $m = 0 / n = 2$ mode with B_{Trot}, are rotating, but the $m = 0 / n > 2$ modes exhibit only slow movement. Phases of m =1 modes show very slow variation, which may not be affected by B_{Trot}. The amplitudes of m = 1 mode in the B_{Trot} applied discharges become slightly smaller than those in the usual discharges with the LM. These are the first results which demonstrate that the LM can be eliminated with B_{Trot}.

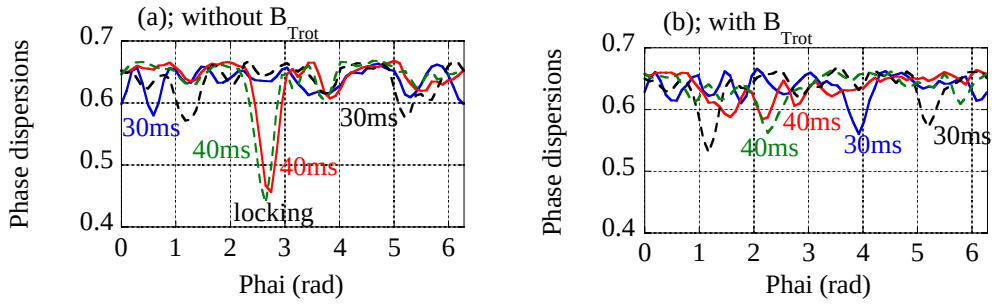

FIG. 2. Phase dispersions at several time points, (a) m = 0 (solid lines) and m = 1 (broken lines) without B_{Trot}, (b) m = 0 (solid lines) and m = 1 (broken lines) with B_{Trot}.

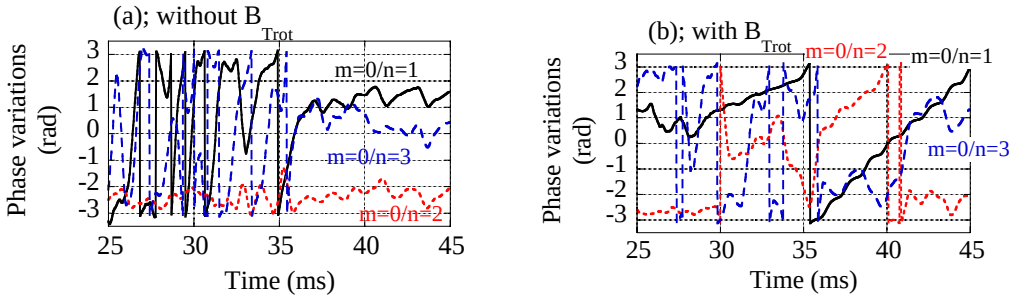

FIG. 3. Phase variations of m = 0 / n = 1-3, (a) without the B_{Trot} case, (b) with the B_{Trot} case.

The required B_{Trot} amplitude to suppress the LM in TPE-RX is about 1.5 % of the poloidal field (B_P). This level is almost the same as the value that an increase of the plasma resistance and a reduction of the soft X-ray signal begin to be observed.

2.3. Pulsed Poloidal Current Drive

To achieve an improvement of the confinement, the pulsed poloidal current drive (PPCD) [8] has been conducted by using the auxiliary toroidal field system and the main reversal toroidal field system (double-pulse PPCD). In the previous single-pulse PPCD, an approximately twofold increase in β_P, τ_E and particle confinement time (τ_p) was achieved [9]. As shown in FIG. 4(a), it is observed that the soft X-ray in the PPCD becomes an order of magnitude larger than that in the standard case. The central electron temperature (T_{e0}) measured by Thomson scattering, the line averaged electron density (n_{el}) measured by a two-color CO_2 interferometer [10] (FIG. 4(b)) and the ion temperature (T_i) measured by a neutral particle energy analyzer (FIG. 4(c)) increase during the PPCD, respectively. Decreases of the magnetic fluctuation and Ohmic input power (P_{Oh}) are also observed. These results for the double-pulse PPCD in TPE-RX show the fivefold increase in τ_E compared to that of the standard case. Since the reversal parameter (F) and Θ change rapidly during the PPCD, the evaluation of τ_E needs an inclusion of the time derivative of the stored energy. We believe that the conventional RFP models are still applicable since the denominator in the calculation of τ_E is well within a finite range.

For the further improvement of τ_E, five-pulse PPCD using the additional three-step reversal capacitor banks has been recently conducted in TPE-RX. During the PPCD, the surface parallel electric field, $E_{//}(a) = (E_\theta B_\theta + E_\phi B_\phi)/B$ [11], is kept positive for longer than before. E_θ and E_ϕ are the surface poloidal and toroidal electric fields, respectively, B_θ and B_ϕ are the surface poloidal and toroidal magnetic fields, and B is the strength of the surface magnetic field. The soft X-ray signal continuously increases without a crash in the five-pulse PPCD case as shown in FIG. 4(a). This result indicates the further improvement of β_P and τ_E compared to in the case of the double-pulse PPCD. The confinement parameters in the five-pulse PPCD are being measured at present.

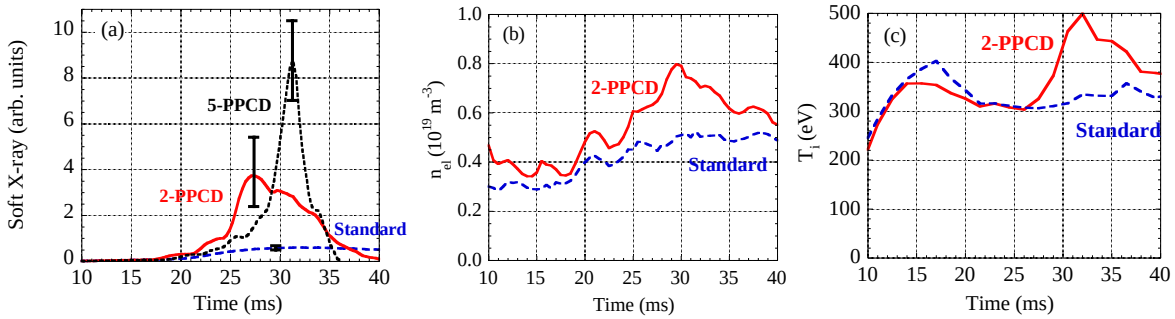

FIG. 4. (a) SXR: solid, broken and dashed lines indicate double-pulse PPCD, standard and five-pulse PPCD discharge cases, respectively, (b) n_{el} and (c) T_i.

2.4. Gus Puffing Experiment

Another improved confinement is obtained in the low I_P/N (high electron density) discharge realized by means of the fast gas puffing technique. The lowest I_P/N value is approximately 2 x 10^{-14} Am, which is comparable to the lowest I_P/N value in RFX. Thus, the gas puffing technique provides a wide range of I_P/N from 2 to 12 x 10^{-14} Am in TPE-RX. When gas puffing is triggered, n_{el} increases by 10 ms in the case of I_P = 300 kA. n_{el} can increase by a factor of 5 from that in the standard operating condition. However, we noticed that central electron density (n_{e0}) measured by Thomson scattering, increases by a smaller factor than the increase ratio of n_{el}, which may indicate that the electron density profile becomes hollow when gas puffing is used. Figure 5 shows β_P and τ_E versus I_P/N. β_P increases as I_P/N decreases. On the other hand, τ_E increases more moderately as I_P/N decreases. The highest values of β_P and τ_E are 22 % and 1.8 ms, respectively, with assumptions of the same ion temperature as the standard discharge for each I_P, and fixed electron and ion temperature profiles. The tendency shown in FIG. 5(a) confirms the β_P scaling versus I_P/N, obtained in many RFP plasmas.

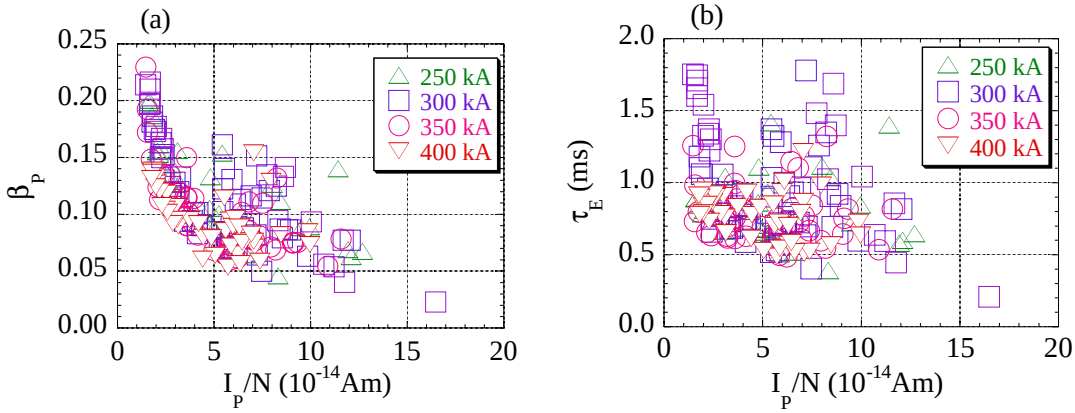

FIG. 5. (a) β_P versus I_P/N, (b) τ_E versus I_P/N.

The radiation fraction measured by a set of bolometer arrays, P_{rad}/P_{Oh}, is approximately 20 % at the flat top of I_P = 300 kA at the high I_P/N value, while the fraction increases to 35 % at the lowest I_P/N (~2 x 10^{-14} Am) as shown in FIG. 6. This result indicates that the lowest I_P/N (the highest density) would be limited by the radiation loss, as is the case at the Greenwald limit in tokamaks.

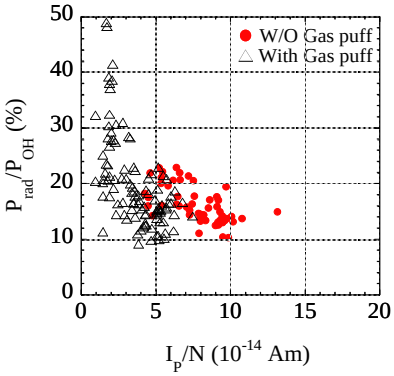

FIG. 6. P_{rad}/P_{Oh} versus I_P/N.

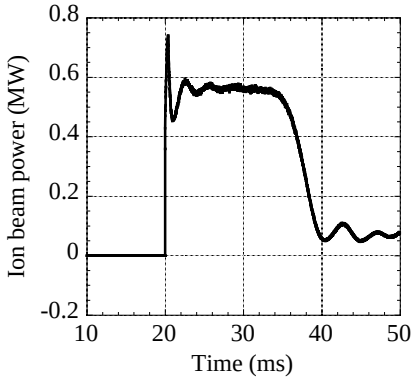

FIG. 7. Typical variation of ion beam power.

3. Neutral Beam Injection to the RFP Plasma

For another active control of the RFP plasma, a neutral beam system with a duration as long as 15 ms and a power as high as 0.4 MW has been developed for the plasma heating, plasma rotation and current drive. The neutral beam is focused by concave-type electrodes. The designed focal length of system is 1500 mm and radius of the electrode is 80 mm. Figure 7 shows typical variations of an ion beam power (P_{beam}). This beam was successfully injected into standard RFP plasmas for the first time. In spite of the small beam power, the slight increase of the soft X-ray signal is indicated in some discharges. Another new neutral beam system of 25 kV, 50A and 30 ms, is being developed for a higher power injection.

4. Conclusion

By applying the rotating toroidal field, the LM can be successfully delayed or even eliminated in the case of $I_P < 250$ kA. This is the first experimental result to demonstrate that the LM can be eliminated by external control. Moreover, the mode analysis indicates that B_{Trot} affects mainly the phase locking, and is unlikely to affect the wall locking of $m = 1$ modes. The result for the double-pulse PPCD gives a fivefold increase in τ_E compared to that of the standard case. The five-pulse PPCD result indicates a further improvement of β_P and τ_E compared to the double-pulse PPCD. The high electron density discharges can be obtained by using the fast gas puffing. The higher values of β_P and τ_E are obtained in the case of the highest electron density. Finally, for another active control of the RFP plasma, the high-power neutral beam injection to the RFP has recently been initiated.

This study is supported by the Ministry of Education, Culture, Sports, Science and Technology, and the Atomic Energy Commission of Japan.

References:

[1] Yagi, Y., et al., Fusion Eng. and Design **45** (1999) 409.
[2] Yagi, Y., et al., Nuclear Fusion **40** (2000) 1933.
[3] Sato, F., et al., Fusion Eng. and Design **54** (2001) 263.
[4] Hirano, Y., et al., Fusion Energy 1998 (Proc. 17th Int. Conf. Yokohama), **1** (2002) 375.
[5] Yagi, Y., et al., Phys. Plasmas **6** (1999) 3824.
[6] Bartiromo, R., et al., Phys. Rev. Lett. **83** (1999) 1779.
[7] Mazur, S., Phys. Plasmas **1** (1994) 3356.
[8] Sarff, J. S., et al., Phys. Rev. Lett. **72** (1994) 3670.
[9] Yagi, Y., et al., Plasma Phys. Control. Fusion **44** (2002) 335.
[10] Canton, A. M., et al., Proc. 28th European Phys. Soc. Conf. Madeira, **25A** (2001) 153.
[11] Chapman, B. E., et al., Phys. Plasmas **9** (2002) 2061.